A CT-based method to compute femur remodelling after total hip arthroplasty

Computer Methods In Biomechanics And Biomedical Engineering: Imaging & Visualization 2021, VOL. 9, NO. 4, 428–437

https://doi.org/10.1080/21681163.2020.1835540

A CT-based method to compute femur remodelling after total hip arthroplasty

L. Iuppariello, Luca Esposito, P. Gargiulo, M. K. Gíslason, H. Jónsson, A. Sarno, L. Cristofolini and P. Bifulco

A CT-based method to compute femur remodelling after Total Hip Arthroplasty

Iuppariello L[a,b], Esposito L[c], Gargiulo P[d], Gíslason MK[d], Jónsson H[e], Sarno A[f], Cristofolini L[g], Bifulco P[bh]*,

[a]Rehabilitation Unit, AORN Santobono Pausilipon Children's Hospital, Italy.
[b]Dept. of Electrical Engineering and Information Technologies (DIETI), University "Federico II" of Naples, Italy.
[c]Dept. of Structures for Engineering and Architecture (DiSt), University "Federico II" of Naples, Italy.
dInstitute for Biomedical and Neural Engineering, Department of Science, Landspıtali University Hospital, University of Iceland, Reykjavik, Iceland.
[e]Department of Orthopaedic Sciences, Landspıtali University Hospital, University of Iceland, Reykjavik, Iceland
[f]INFN sect. of Napoli & Dept. of Physics, University "Federico II" of Naples, Italy.
[g]Dept. of Industrial Engineering, University of Bologna, Italy
hIstituti Clinici Scientifici Maugeri SpA – società benefit, Pavia, Italy

*correspondng author: pabifulc@unina.it

Abstract

Bone remodelling after total hip arthroplasty has been largely observed and investigated. Most studies rely on projective images and only few obtain 3D information with limited spatial resolution. This study proposes a method to provide quantitative, 3D high-resolution data about femur bone density variations, by means of CT volume processing. This would offer a tool for further research and clinical studies. Five patients subjected to primary, cementless total hip arthroplasty were considered. Calibrated CT volumes were acquired before, just after surgery, and one year later. Bone remodelling hinders accurate alignment of femur volumes acquired after a year, instead, prosthesis stem remains unchanged. Thus, after metal artifact reduction, prosthesis was segmented, and stem-based accurate alignment was obtained. A test to exclude prosthesis migration was performed by considering specific femur anatomical landmarks. Bone density error due to artifact reduction and realignment were estimated. Quantitative differences in bone mineral density were computed for each voxel, providing a resolution of about 1 mm. Preliminary results showed that the femur underwent consistent remodelling after a year. Widespread bone density losses appeared in those areas where stress shielding is normally expected, particularly about the calcar. Conversely, distal areas with clear stem-bone contact showed considerable density gains.

Keywords: Total Hip Arthroplasty, femur bone remodelling, CT image processing, prosthesis rigid realignment

1. Introduction

Total Hip Arthroplasty (THA) produces significant variations of the stress distribution in the femur, which adapts after implantation. Remodelling [1] depends on implant size, geometry, mechanical properties and fixation type (i.e. cemented or cementless). Uncemented fixation has gained wide acceptance and is the first choice for younger and more active patients [2,3]. Cementless femoral stems have a lower risk of aseptic loosening failure than cemented femoral stems in younger patients [4-7]. Accurate fit and fill in the proximal femur are considered important to achieve physiological load transfer [8].

Prosthesis implantation inevitably changes the load distribution in the host bone, and the femur remodels accordingly. Bone remodels itself in response to load (Wolff's law). After THA diffuse reductions in bone density appears around the prosthesis stem because of *stress shielding* [9-14]. After primary THA rapid bone loss occurs during the first months and it progress more slowly in subsequent years [15]. Bone loss in the calcar area up to one year, is 22.9% in the uncemented and 24.5% in the cemented prosthesis [16]. Bone Mineral Density (BMD) can be considered a good indicator of bone quality and its change over time [17]. Bone density loss leads to local bone weakening and fracture risk increases. In general, missing implant-bone contact or osteolysis around the stem might lead to failure of the prosthesis after few years [18,19]. Furthermore, bone loss makes revision surgery more critical and less successful. But prosthesis also produces bone density gains at specific locations (e.g. at the preferential support points of the prosthesis stem). In such areas, bone density drastically increases in response to the increased mechanical stimuli.
Bone remodelling also depends on patient-related factors such as gender, age, initial femoral bone stock, patient activity and general health conditions, as well as prosthesis-related factors, such as type of fixation, stem length, stiffness, femoral bone preparation [20].

Although the large majority of THA is correctly performed, a significant percentage of patients undergoing THA requires revision within 10 to 15 years after surgery [22]. Aseptic loosening, instability, associated osteolysis and infection are reported as the major reason for implant failure in 71% of cases [23]. The postoperative reduction of the periprosthetic bone density after implantation of uncemented and cemented [13] stems is considered a main problem in orthopaedic surgery. Therefore, it would be advantageous to estimate patient's BMD prior to performing THA surgery [24,25], but these measurements are not a standard today. In general, there is interest to accurately monitor bone remodelling as well. Bone resorption cause aseptic loosening, but multifactorial events concur: wear-debris induced osteolysis, excessive interface micromotions,

and stress shielding concur (with other factors) to a negative sequence of events [26,27]. Therefore, it is not still quite clear to what extent stress shielding alone would lead to implant failure [28].

Minimizing bone loss after THA is desirable, and bisphosphonate treatment can help to reduce acute periprosthetic bone loss [29]. However, bisphosphonates show severe detrimental side effects such as heterotopic ossifications [30] and their use is therefore limited to extreme cases.

Stress shielding has extensively been studied *in vitro* [31-35], but actual stress shielding consequences have to be demonstrated *in vivo*. Evaluation of bone remodelling after THA is often evaluated measuring BMD by means of Dual-Energy X-ray Absorptiometry (DEXA) [36-38], but only 2D projections are available. Usually, seven macro-areas (i.e. Gruen zones [39]) adjacent to the implant are considered. Inherently, DEXA analysis cannot provide the specific, 3D information (e.g. complete circumferential data) on local variations of femur BMD.

In the past, some attempts to use three-dimensional imaging techniques to study more thoroughly the changes in bone density were tried. With recent improvements in metal artifact reduction techniques, CT are more and more used for accurate analysis of bone remodelling [40-45]. In particular, quantitative CT-based osteodensitometry were proposed to get more detailed information on BMD at different levels of the femur by analyzing the cross-sectional CT images [46-48]. Another study [49] proposed an even more detailed BMD analysis by means of CT data, but without specifically addressing the metal artifact problem, and only focusing on patients with cemented implants.

In summary, while stress shielding and the consequent bone remodelling has been extensively assessed in the past in qualitative terms, a method is still missing to enable a quantitative, volumetric measurement of bone resorption or apposition around a cementless stem. This would allow quantifying bone remodelling and effects of stress shielding over time.

The objective of this study is to develop and test a method able to quantitatively and accurately measure femur bone density changes through time. This method provides a research tool for a large cohort investigation and further studies. CT volumes of real patients who underwent THA were recorded just before, after surgery, and after one year. Thanks to the prospective nature of this study, consistent and completed dataset were available. By comparing the two CT scan of the operated femurs, a three-dimensional, quantitative, high-resolution map of BMD changes is provided.

2. Materials and methods

Patient CT scans taken at different times post-operatively were compared. The process included reduction of the metal artefacts, registration of the CT scans taken at different times (this process

included segmentation, the actual registration, resampling and smoothening), a check for the lack of excessive implant migrations, and the actual comparison between the scans. In addition, in this study we performed a dedicated study to quantify the uncertainty propagating from the different steps to the final HU values.

2.1. CT - image acquisition

The patient CT data were selected from a previous study [50,51]. Five patients who underwent a primary hip replacement, implanted with Spotorno cementless implant were involved in this study (Table 1).

Patient	Gender	Age	Weight [Kg]	Operated Side	Implant Type
GSF63	F	63	96	Left	Cementless
BEM52	M	52	95	Left	Cementless
GMM43	M	43	87	Left	Cementless
BTM21	M	66	66	Right	Cementless
BJF59	F	59	89	Right	Cementless

Table 1 Patients enrolled in the study

Patients' volumes were acquired using a spiral CT Scan Philips Brilliance 64 slices in Reykjavik. X-ray tube voltage was set to 120 KVp, slice thickness is 1 mm (with increments of 0.5 mm) while pixel size was 0.6 by 0.6 mm (voxel volume = 0.36 mm^3), each slice was 512x512 pixels, 12-bit precision grey values (Hounsfield Units range from -1024 to 3072). CT scan started from anterior superior iliac spine and ended approximately to the middle of the femur shaft.

All the CT scans were calibrated using a Quasar Multi-Purpose Body Phantom to evaluate the relationship between HU and BMD [52]. Patient's CT scans were acquired before surgery (hereafter coded as: "pre-op"), within 24 hours after surgery ("24h"), and 1 year later ("1yr").

2.2. Metal Artefact Reduction (MAR)

Presence of metal prosthesis causes considerable artifacts in CT images [53,54]. Typical streaks propagating from the implant produces a large amount of noise in the surrounding tissues and in particular in femur bone hindering further analysis. Therefore, a post-processing, metal deletion technique (MDT) [55] was performed to reduce the artifacts in post-operative CT. Figures 1 (a) and (b) provides an example of the algorithm performance.

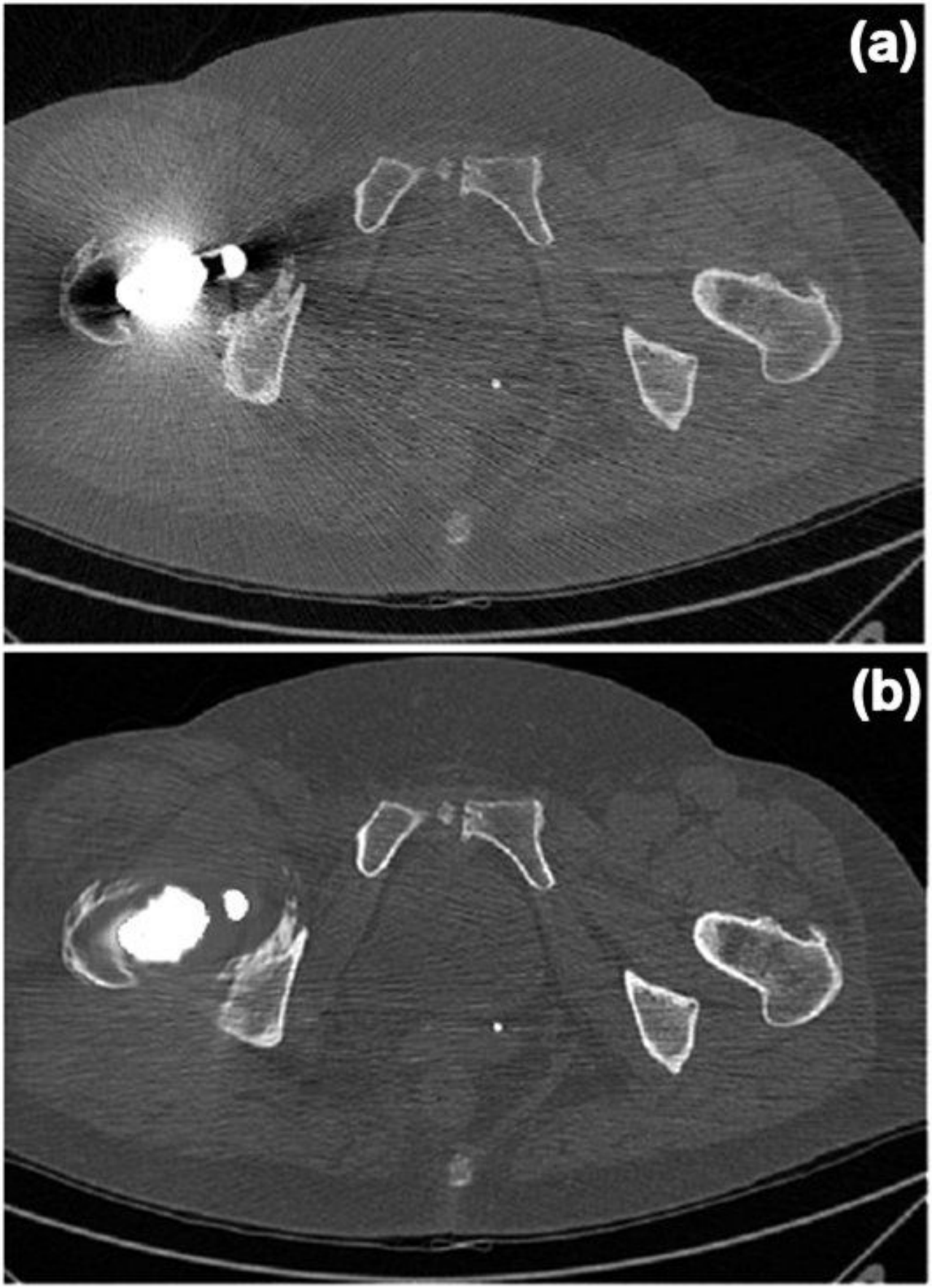

Figure 1: (a) a raw CT slice enclosing the metal prosthesis ; (b) the same slice after Metal Artifact Reduction

2.3. Registration of 24h – 1yr CT scans

The 24h and 1yr CT datasets cannot be straightforward compared because they were acquired in different times and conditions (i.e. patient positioning have varied, and bone have changed). Patients' 24h and 1yr femurs must be registered before further analysis. The following, multi-step rigid 3D registration process was applied.

As a first step, once the metallic artefact was suppressed, the operated femur was segmented from both, 24h and 1yr CT volumes: initially, bone tissues were roughly segmented by means of thresholding (voxel with HU values larger than 260 were pre-selected). As a second step, the segmented, binary volumes were smoothed using 3D binary operators. Once the femur (including the prosthesis) was selected, the outer volume (i.e. all its surroundings) was arbitrarily set as air (HU=-1024). At this stage, volumes containing only the operated femur and the prosthesis were available (see Fig. 2a). As a third step, the two CT volumes (24h and 1yr) were aligned by applying a surface registration. Rather than using the surface of the entire femur, the stem surface was considered because the bone has possibly changed during the year. The stem was segmented, and its surface was reconstructed in both 24h and 1yr volumes. The 24h and 1yr surfaces were rigidly registered by means of the Iterative Closest Point algorithm [56], which uses similarity and affine transforms. As a fourth step, the registered 1yr volume was re-sampled (by means of linear interpolation) to match the voxeling of the 24h volume. Therefore, a pixel-to-pixel correspondence between the 24h and the aligned 1yr CT volumes was available (see Fig. 2b).

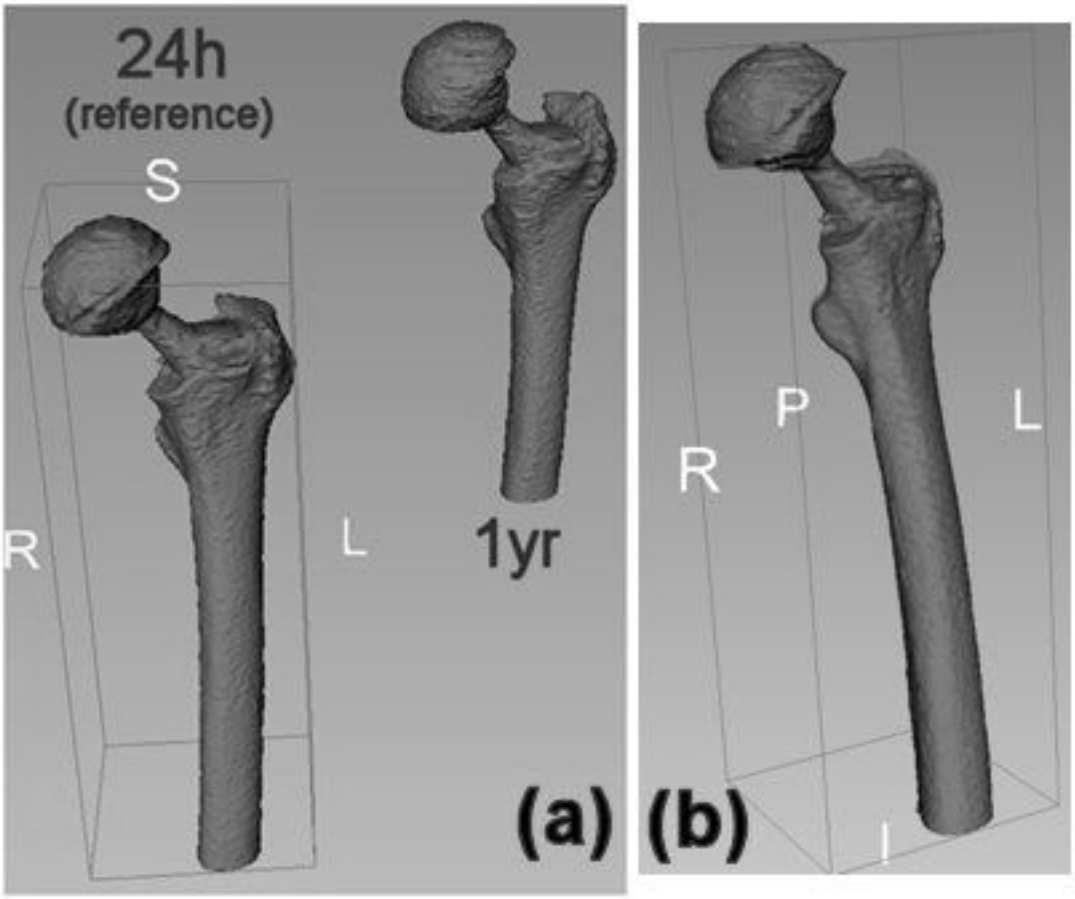

Figure 2: (a) a femur 24 hour after the surgical implant (on the left) and the same femur after 1 year (on the right): the two femurs are not aligned ; (b) the two femurs aligned.

Then, in order to reduce the interpolation and alignment errors and to preserve edges, the CT volumes were 3D low-passed filtered. A simple, conditioned-average smoothing filter (sized 3x3x3 pixels, corresponding to 1.8 by 1.8 by 3.0 mm) was applied. Only the voxels, whose difference with the central voxel were less than 600 HU (an arbitrary threshold value), were used to compute the average. Very steep edges (e.g. bone-prosthesis, bone-outside) were preserved, while uniform regions were averaged (e.g. inside the bone). As example Figure 3 show the resulting volumes at this stage.

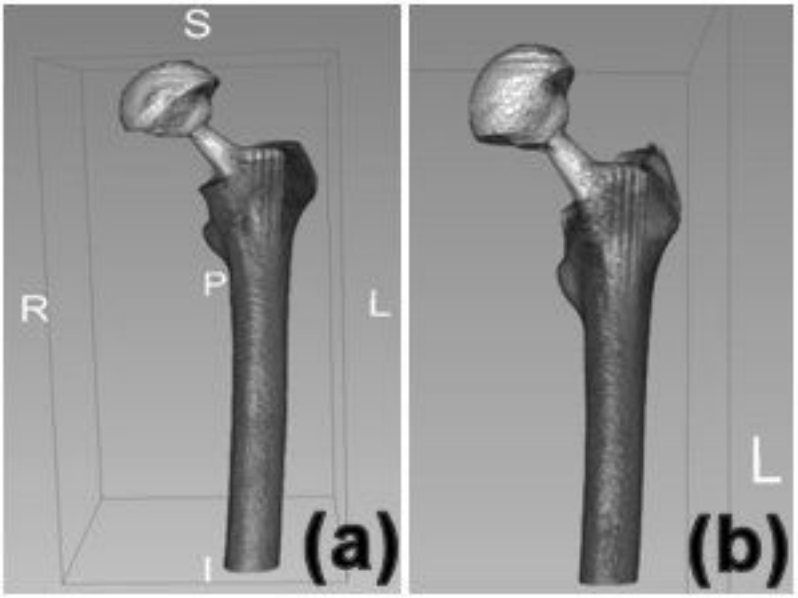

Figure 3: an example of two aligned femurs after the conditioned-average smoothing filter: (a) the femur 24 hour after the surgical implant ; (b) the same femur after 1 year.

2.4. Tests to quantify migration

Since the femur alignment procedure relied on the prosthesis geometry, the cases where the stem significantly migrated must be excluded. The relative positioning between the prosthesis stem and the femur must be somehow estimated between 24h – 1yr volumes. To this end, starting from the aligned femurs, the external surfaces of the 24h and the 1yr femurs were extracted. Again, the Iterative Closest Point rigid registration procedure was applied to these surfaces and the correspondent roto-translation matrix was computed. Ideally, if there was no migration, the resulting displacements and rotations should be zero, but practically this cannot happen exactly because the bone has reshaped. Error thresholds of 2 mm for displacements a 1 degree for rotations were empirically set (according to the CT resolution) to verify the absence of migration. The errors computed for all the patients resulted below these thresholds and then the occurrence of prosthesis migration was excluded.

An additional, redundant test was also carried out to confirm the reliability of the former procedure: three specific anatomic landmarks (i.e. The entrance of the arterial foramen in the femur shaft; The most posterior protuberance of the lesser trochanter; The most posterior anterior protuberance of the greater trochanter) were manually identified and selected on both 24h and 1yr volumes. Their relative locations with respect to the prosthesis were evaluated. Again, displacements and rotations were confined below the aforementioned thresholds.

2.5. CT processing errors assessment

Patients' pre-operative volumes were used to evaluate the errors associated to the metal artefact suppression and realignment procedures. The 24h CT volume (after metal artefact suppression) was compared with the pre-op CT scan. As only few days passed between the two scans, we can assume that the bone has not changed. The difference in HU between these two volumes is therefore a measure of the uncertainty associated to the CT volume manipulations.

Once again there is the need to align the two femurs, but the prosthesis is not present in both volumes. The procedure adopted for this rigid alignment consists of two stages. A first rough 3D registration based on anatomic landmarks was followed by a finer rigid-global registration based on HU similarity index. The three aforementioned anatomic landmarks were manually selected on both femurs and the rigid roto-translation was computed. Then, a finer adjustment was obtained by minimizing the HU differences in all the voxels belonging to the compact bone. This fine registration is based on the Mattes mutual information registration metric [57]. Finally, the aligned, post-operative femur was opportunely re-sampled (by means of linear interpolation). Differences in HU of corresponding voxels belonging to the pre-operative and the 24h femur were computed (see Fig. 4). The error followed a Gaussian distribution (Kolmogorv-Smirnov test, p=0.999), with mean close to 0 HU and standard deviation about 150 HU. This has suggested to consider bone HU changes significant only if they exceed the value of 200 HU.

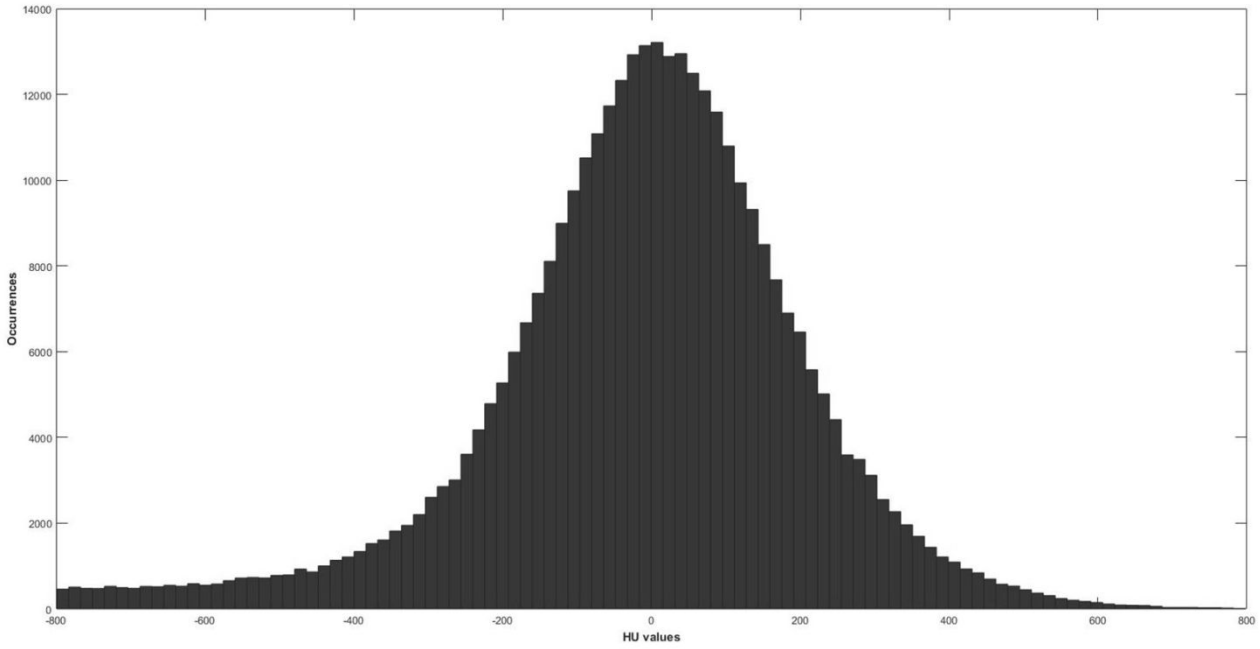

Figure 4: histogram of the HU differences of correspondent voxels belonging to the pre-operative and the 24h femur.

2.6. Quantification of bone changes

A 3D, high-resolution map of the femoral bone HU differences was obtained. For each voxel, the bone density 1-year difference was available. The HU differences were grouped in five regions solely to provide more concise and intuitive representation of bone remodelling (see table II for colours). As specified above, HU differences between -200 and +200 were associate to unmodified bone. HU differences between -1200 and -200 were associated to bone tissue that lost mineral content, while greater negative values (i.e. HU differences <-1200) were associated to complete bone loss. Conversely, HU differences between +200 and +1200 were associated to bone tissue that gained mineral content, while greater positive values (i.e. HU differences > +1200) were associated to newly formed bone. The coloured data were superimposed on the gray-scale images in order to better appreciate anatomical details.

Region	HU range	Colour
Eroded	[-3000; -1201]	Red
Density Loss	[-1200; -201]	Orange
Unmodified bone	[-200; +200]	transparent
Density Gain	[201;1200]	Light green
New-born	[1201; 3000]	Dark green

Table 2 The selected HU ranges and the corresponding colours adopted to map bone remodelling.

In addition, bone loss-gain parameters were estimated within the Gruen zones (Zone 1: Greater trochanter; Zone 2: Proximal lateral; Zone 3: Distal Lateral; Zone 4: Sub prosthetic peak; Zone 5: Distal Medial; Zone 6: Proximal Medial; Zone 7: Calcar), as shown in Figure 5.

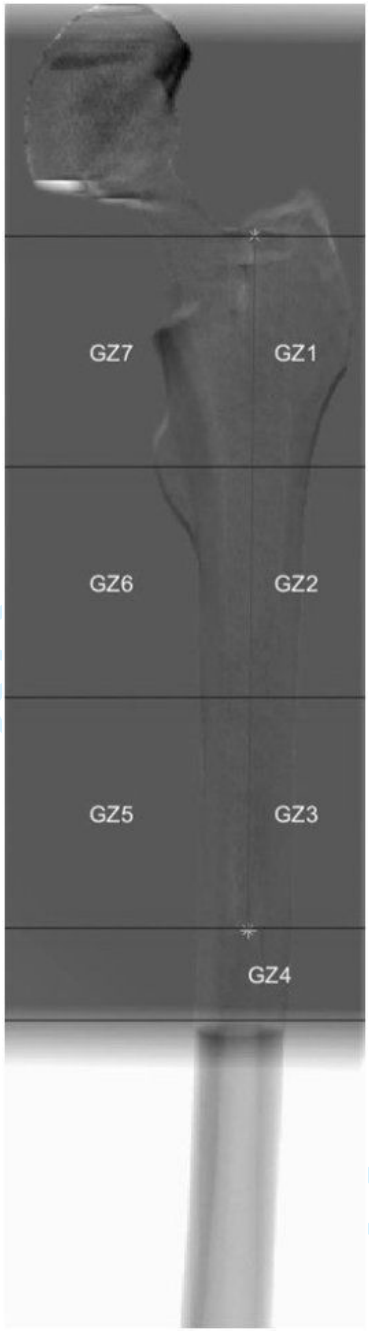

Figure 5: an example of the Gruen zones (1 to 7) on a projection of the realigned femurs

3. Results

The entire procedure was successfully applied to the five real patients' datasets., Figure 6 shows, for each patient (labelled from (a.) to (e.)) two axial sections in correspondence of the calcar (labelled as (.1)) and of the prosthesis distal tip (labelled as (.2)) particularly meaningful for bone remodelling after THA. For each sub-image on the left the pseudo-coloured 2D slices are presented while on the right the corresponding cutting plane is showed.

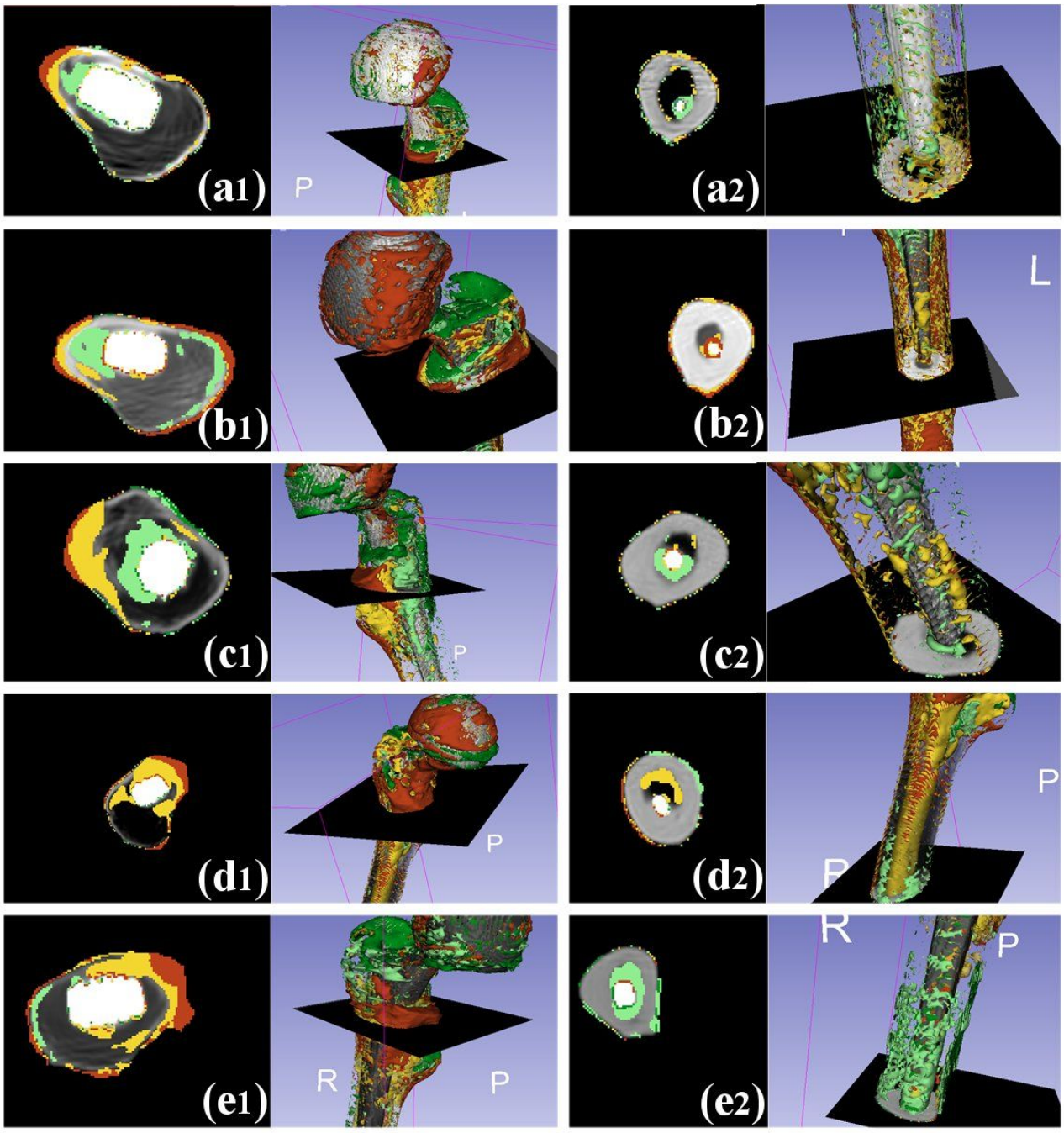

Figure 6: Examples of the 3D differential representation. Each patient is labeled with a letter from (a.) to (e.). Axial sections in correspondence of the calcar are labeled as (.1) and axial sections at the prosthesis distal tip are labeled as (.2). For each sub-image the axial section is represented on the left and the corresponding 3D map with the cutting plane is represented on the right.

In addition to the concise illustration of the Table II regions, it is possible to obtain a much more detailed and continuous representation of bone density variations. As example, Figure 7(b) shows

the 1-year variations of the HU along an arbitrarily chosen segment (depicted as a white arrows) belonging to the slice shown in Figure 7(a).

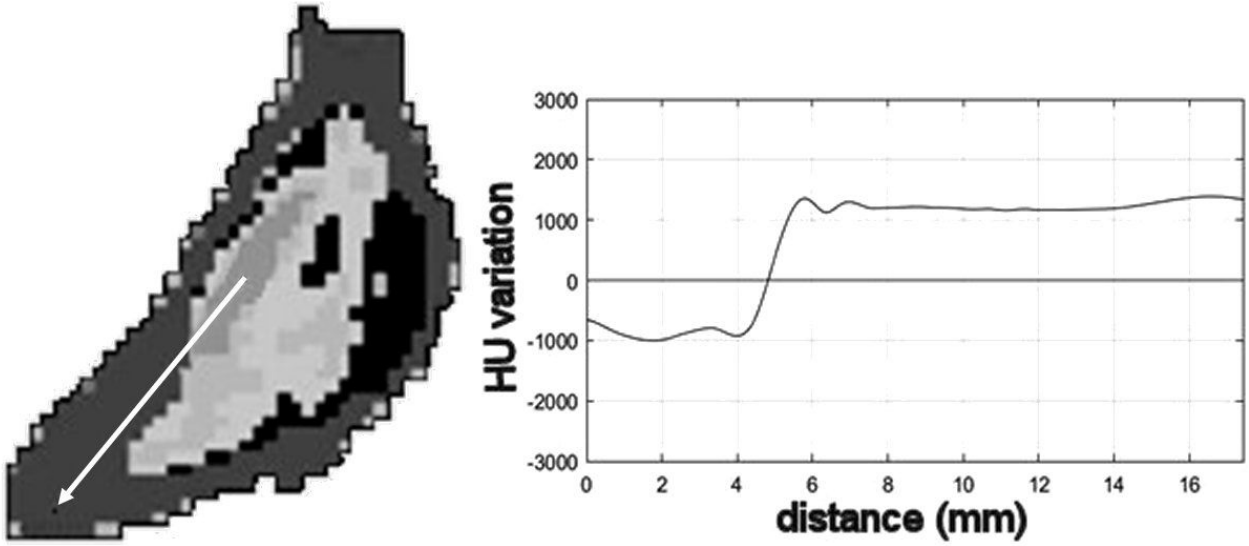

Figure 7: (a) an example of a slice (cutting the great trochanter) on which a segment was arbitrarily chosen and indicated by a white arrow: (b) The HU variations along the segment showed as the white arrow in panel (a)

Cumulative bone density variations (averaged on all patients) are reported in table 3 for each Gruen zone. The variations were computed as mean percentage of HU changes.

Region	GZ1	GZ2	GZ3	GZ4	GZ5	GZ6	GZ7
Eroded (%)	4	4	2	2	2	4	6
Bone Loss (%)	5	10	7	9	9	15	16
Unmodified bone (%)	**78**	**75**	**82**	**82**	**80**	**68**	**58**
Bone Gain (%)	9	8	6	4	5	9	13
New-born (%)	2	1	1	1	3	1	5

Table 3 Percentage of variations in the Gruen Zone = number of voxels that are in the considered ROI / number of voxels that are in the considered Gruen zone. * 100

In general, according to these results we can say that the bone, after one year from the total hip arthroplasty, presents a significant remodelling related to all Gruen zones.

4. Discussion

This study proposes a methodology for obtaining an accurate, patient-specific, 3D map of the femur bone density variations after THA. Different 3D rigid realignments of both the prosthesis and the

femur were adopted to achieve a reliable and robust analysis tool to accurately evaluate bone remodelling. It proposes and test the feasibility of the methodological approach and does not claim to provide exhaustive results of remodelling map on a large patients' cohort.

Preliminary results related to the five patients indicate that the femur, even after only one year, resulted enough modified. In particular, the external part of the calcar shows great losses and even bone resorption, in line with many other studies [58-61]. On the contrary, in the calcar region adjacent to prosthesis, a significant increase in bone density was found: this bone reinforcement is supposed to support the great mechanical load generated at this point by the prosthesis. Similarly, a particular intense bone growth resulted close to the distal tip of the prosthesis stem. Generalised bone density losses along the bone shaft appeared as result of the stress shielding phenomenon. In addition, cumulative results corresponding to the Gruen zones were presented to allow comparative studies.

In conclusion, the proposed methodology offers a very accurate tool for analyzing bone remodelling by providing bone density differences with a resolution comparable to that of CT equipment. This approach, if applied to more patients, would provide a better understanding of the bone remodelling. Furthermore, the proposed methodology could be extended to the case of cemented prostheses. Finally, the objective results provided by the proposed methodology could be of help in prostheses design and assessment.

5. Acknowledgements

Authors are thankful to Dr. Jonathan Pitocchi and Dr. Andrea Menichetti who contributed to some stages of this project.

Competing interests: None declared

Funding: None

Ethical approval: VSN 13-127-S1

6. References

[1] Tavakkoli Avval P, Klika V, Bougherara H. Predicting bone remodeling in response to total hip arthroplasty: computational study using mechanobiochemical model. J Biomech Eng. 2014; 136(5):051002. DOI: 10.1115/1.4026642.

[2] Schmidutz F, Grote S, Pietschmann M, Weber P, Mazoochian F, Fottner A, Jansson V. Sports activity after short-stem hip arthroplasty. Am J Sports Med 2012; 40(2):425–432. DOI: 10.1177/0363546511424386

[3] Kim YH, Kim JS, Park JW, Joo JH. Comparison of total hip replacement with and without cement in patients younger than 50 years of age: the results at 18 years. J Bone Joint Surg Br. 2011; 93:449–455. DOI: 10.1302/0301-620X.93B4.26149

[4] Eskelinen A, Remes V, Helenius I. Total hip arthroplasty for primary osteoarthrosis in younger patients in the Finnish arthroplasty register. 4,661 primary replacements followed for 0–22 years. Acta Orthop. 2005; 76(1):28-41. DOI: 10.1080/00016470510030292

[5] Mäkelä KT, Eskelinen A, Pulkkinen P, Paavolainen P, Remes V. Total hip arthroplasty for primary osteoarthritis in patients fifty-five years of age or older. An analysis of the Finnish arthroplasty registry. J Bone Joint Surg Am. 2008; 90(10):2160-2170. DOI: 10.2106/JBJS.G.00870

[6] Mäkelä KT, Matilainen M, Pulkkinen P. Failure rate of cemented and uncemented total hip replacements: register study of combined Nordic database of four nations. BMJ. 2014;348:f7592. DOI: 10.1136/bmj.f7592

[7] Australian Orthopaedic Association. Hip and knee arthroplasty. Annual Report of the National Joint Replacement Registry. 2012.

[8] Laine HJ, Puolakka TJS, Moilanen T, Pajamäki KJ, Wirta, J, Lehto MUK. The effects of cementless femoral stem shape and proximal surface texture on 'fit-and-fill' characteristics and on bone remodelling. International Orthopaedics. 2000; 24(4):184-190. DOI: 10.1007/s002640000150

[9] Fagan MJ, Lee AJ. Role of the collar on the femoral stem of cemented total hip replacements. J Biomed Eng. 1986; 8(4):295-304. DOI: 10.1016/0141-5425(86)90061-0

[10] Engh CA. Hip arthroplasty with a Moore prosthesis with porous coating. A five-year study. Clin Orthop Relat Res. 1983; 176:52-66.

[11] Engh CA, Bobyn JD. Principles, techniques, results, and complications with a porous-coated sintered metal system. Instr Course Lect. 1986; 35:169-83.

[12] Engh CA, Bobyn JD, Glassman AH. Porous-coated hip replacement. The factors governing bone ingrowth, stress shielding, and clinical results. J Bone Joint Surg Br. 1987;69(1):45-55.

[13] Dan D, Germann D, Burki H, Hausner P, Kappeler U, Meyer RP, Klaghofer R, Stoll T. Bone loss after total hip arthroplasty. Rheumatol Int. 2006; 26(9):792-8. DOI: 10.1007/s00296-005-0077-0

[14] Damborg F, Nissen N, Jørgensen HR, Abrahamsen B, Brixen K. Changes in bone mineral density (BMD) around the cemented Exeter stem: a prospective study in 18 women with 5 years follow-up. Acta Orthop. 2008; 79(4):494-8. DOI: 10.1080/17453670710015481

[15] Boldt JG, Cartillier JC, Machenaud A, Vidalain JP. Long-term Bone Remodeling in HA-coated Stems: A Radiographic Review of 208 Total Hip Arthroplasties (THAs) with 15 to 20 Years Follow-up. Surg Technol Int. 2015; 27:279-86.

[16] Venesmaa P, Vanninen E, Miettinen H, Kröger H. Periprosthetic bone turnover after primary total hip arthroplasty measured by single-photon emission computed tomography. Scand J Surg. 2012; 101(4):241-8. DOI: 10.1177/145749691210100404

[17] Soininvaara, T. Miettinen, J. Hannu, S.Jurvelin, M. Alhava, Kruger P. Changes in bone mineral density of the proximal femur after total knee arthroplasty. The Journal of arthroplasty 2000; 7(4):424– 431. DOI: 10.1054/arth.2000.4639

[18] Kobayashi S, Saito N, Horiuchi H, Iorio R, Takaoka K. Poor bone quality or hip structure as risk factors affecting survival of total-hip arthroplasty. Lancet. 2000; 355(9214):1499-1504. DOI: 10.1016/S0140-6736(00)02164-4

[19] Nishii T, Sugano N, Masuhara K, Shibuya T, Ochi T, Tamura S. Longitudinal evaluation of time related bone remodeling after cementless total hip arthroplasty. Clin Orthop Relat Res. 1997; 339:121-131. DOI: 10.1097/00003086-199706000-00017

[20] Hananouchi T, Sugano N, Nishii T, Nakamura N, Miki H, Kakimoto A, Yamamura M, Yoshikawa H. Effect of robotic milling on periprosthetic bone remodeling. J Orthop Res. 2007; 25(8):1062-1069. DOI: 10.1002/jor.20376

[21] Improta G, Balato G, Romano, Carpentieri F, Bifulco P, Russo AM, Donato R, Triassi M, Cesarelli M. Lean Six Sigma: A new approach to the management of patients undergoing prosthetic hip replacement surgery. J Eval Clin Pract, 2015; 21:662-672, https://doi.org/10.1111/jep.12361

[22] Havelin LI, Espehaug B, Vollset SE, Engesaeter LB. Early aseptic loosening of uncemented femoral components in primary total hip replacement. A review based on the Norwegian Arthroplasty Register. J Bone Joint Surg Br. 77(1):11-17

[23] Herberts P, Malchau H. Long-term registration has improved the quality of hip replacement: a review of the Swedish THR Register comparing 160,000 cases. Acta Orthop Scand. 2000; 71(2):111-121. DOI: 10.1080/000164700317413067

[24] Venesmaa PK, Kröger HP, Jurvelin JS, Miettinen HJ, Suomalainen OT, Alhava EM. Periprosthetic bone loss after cemented total hip arthroplasty: a prospective 5-year dual energy radiographic absorptiometry study of 15 patients. Acta Orthop Scand. 2003; 74(1):31-36. DOI: 10.1080/00016470310013617

[25] Huiskes R, Weinans H, van Rietbergen B. The relationship between stress shielding and bone resorption around total hip stems and the effects of flexible materials. Clin Orthop Relat Res. 1992; 274:124-134.

[26] Varnum C. Outcomes of different bearings in total hip arthroplasty - implant survival, revision causes, and patient-reported outcome. Dan Med J. 2017; 64(3): B5350

[27] Tsertsvadze A, Grove A, Freeman K, Court R, Johnson S, Connock M, Clarke A, Sutcliffe P. Total hip replacement for the treatment of end stage arthritis of the hip: a systematic review and meta-analysis. PLoS One. 2014; 9(7):e99804. DOI: 10.1371/journal.pone.0099804

[28] Harris WH. Will stress shielding limit the longevity of cemented femoral components of total hip replacement? Clin Orthop Relat Res. 1992; 274:120-123.

[29] Prieto-Alhambra D, Javaid MK, Judge A, Maskell J, Kiran A. De Vries F, Cooper C, Arden NK. Fracture risk before and after total hip replacement in patients with osteoarthritis potential benefits of bisphosphonate use. Arthritis and Rheumatism. 2011; 63(4):992-1001. DOI: 10.1002/art.30214

[30] Eriksen EF, Halse J, Moen MH. New developments in the treatment of osteoporosis. Acta Obstet Gynecol Scand. 2013; 92(6):620-36. DOI: 10.1111/j.1600-0412.2012.01473.x

[31] Cristofolini L, Bini S, Toni A. In vitro testing of a novel limb salvage prosthesis for the distal femur. Clinical Biomechanics. 1998; 13(8):608-615. DOI: 10.1016/S0268-0033(98)00024-2

[32] Cristofolini L, Viceconti M. In vitro stress shielding measurements can be affected by large errors. Journal of Arthroplasty. 1999; 14(2):215-219. DOI: 10.1016/S0883-5403(99)90129-8

[33] Esposito L, Bifulco P, Gargiulo P, Fraldi M. Singularity-free finite element model of bone through automated voxel-based reconstruction Singularity-free finite element model of bone through automated voxel-based reconstruction Comput Methods Biomech Biomed Engin. 2016; 19(3):257-262. DOI: 10.1080/10255842.2015.1014347

[34] Volpe V, Miraglia C, Esposito L, Fraldi M. X-ray based technique for estimating bone fracture risk. Proceedings of the 2nd WSEAS International Conference on Biomedical Electronics and Biomedical Informatics. 2009; 244-246.

[35] Fraldi M, Esposito L, Perrella G, Cutolo A, Cowin SC. Topological optimization in hip prosthesis design. Biomech Model Mechanobiol. 2009; 9(4):389–402. DOI: 10.1007/s10237-009-0183-0

[36] Tapaninen T, Kröger H, Venesmaa P. Periprosthetic BMD after cemented and uncemented total hip arthroplasty: a 10-year follow-up study. J Orthop Sci. 2015; 20(4):657-62. DOI: 10.1007/s00776-015-0722-8

[37] Rahmy AI, Tonino AJ, Tan W, Ter Riet G. Precision of dual energy X-ray absorptiometry in determining periprosthetic bone mineral density of the hydroxyapatite coated hip prosthesis. Hip Int. 2000; 10:83–90.

[38] Chun KJ. Bone densitometry. Semin Nucl Med. 2011; 41(3):220-8.

[39] Gruen T A, McNeice GM, Amstutz HC. Modes of failure of cemented stem type femoral components: a radiographic analysis of loosening. Clin Orthop Relat R. 1979; 141:17-27.

[40] Puri L, Wixson RL, Stern SH, Kohli J, Hendrix RW, Stulberg SD. Use of helical computed tomography for the assessment of acetabular osteolysis after total hip arthroplasty. J Bone Joint Surg Am. 2002; 84-A(4):609-14.

[41] Egawa H, Ho H, Huynh C, Hopper RH, Jr, Engh CA, Jr, Engh CA. A three-dimensional method for evaluating changes in acetabular osteolytic lesions in response to treatment. Clin Orthop Relat Res. 2010; 468(2):480-90. DOI: 10.1007/s11999-009-1050-0

[42] Cahir JG, Toms AP, Marshall TJ, Wimhurst J, Nolan J. CT and MRI of hip arthoplasty. Clin Radiol 2007; 62:1163–1171. DOI: 10.1016/j.crad.2007.04.018

[43] Howie DW, Neale SD, Stamenkov R, McGee MA, Taylor DJ, Findlay DM. Progression of acetabular periprosthetic osteolytic lesions measured with computed tomography. J Bone Joint Surg Am. 2007; 89:1818–1825. DOI: 10.2106/JBJS.E.01305

[44] Kress AM, Schmidt R, Vogel T, Nowak TE, Forst R, Mueller LA. Quantitative computed tomography-assisted osteodensitometry of the pelvis after press-fit cup fixation: a prospective 10-year followup. J Bone Joint Surg Am 2011; 93:1152–1157. DOI: 10.2106/JBJS.J.01097

[45] Sandgren B, Crafoord J, Garellick G, Carlsson L, Weidenhielm L, Olivecrona H. Computed tomography vs. digital radiography assessment for detection of osteolysis in asymptomatic patients with uncemented cups: a proposal for a new classification system based on computer tomography. J Arthroplasty. 2013; 28(9):1608-13. DOI: 10.1016/j.arth.2013.01.029

[46] Pitto RP, Bhargava A, Pandit S, Walker C, Munro JT. Quantitative CT-assisted osteodensitometry of femoral adaptive bone remodelling after uncemented total hip arthroplasty. Int Orthop. 2008; 32(5): 589-595. DOI: 10.1007/s00264-007-0389-7

[47] Pitto RP, Hayward A, Walker C, Shim VB. Femoral bone density changes after total hip arthroplasty with uncemented taper-design stem: a five year follow-up study. International Orthopaedics (SICOT). 2010; 34:783-787. DOI: 10.1007/s00264-009-0884-0

[48] Arachchi S, Pitto RP, Anderson IA, Shim VB. Analyzing bone remodeling patterns after total hip arthroplasty using quantitative computed tomography and patient-specific 3D computational models Quant Imaging Med Surg. 2015; 5(4):575-582.

[49] Burchard R, Leppek R, Schmitt J, Lengsfeld M. Volumetric measurement of periprosthetic bone remodeling: prospective 5 years follow-up after cemented total hip arthroplasty. Arch Orthop Trauma Surg. 2007; 127(5):361-8. DOI: 10.1007/s00402-007-0293-z

[50] Gargiulo P, Edmunds KJ, Gíslason MK, Latour C, Hermannsson Þ, Esposito L, Bifulco P, Cesarelli M, Fraldi M, Cristofolini L, Jónsson H Jr. 2018. Patient-specific mobility assessment to monitor recovery after total hip arthroplasty. Proc Inst Mech Eng H. 232(10):1048-1059. DOI: 10.1177/0954411918797971

[51] Esposito L, Bifulco P, Gargiulo P, Gíslason MK, Cesarelli M, Iuppariello L, Jónsson H, Cutolo A, Fraldi M. Towards a patient-specific estimation of intra-operative femoral fracture risk. Comput Methods Biomech Biomed Engin. 2018; 21(12):663-672 DOI: 10.1080/10255842.2018.1508570

[52] Gargiulo P, Petursson T, Magnusson B, Bifulco P, Cesarelli M, Izzo GM, Magnusdottir G, Halldorsson G, Ludvigsdttir GK, Tribel J, Jonsson H. Assessment of Total Hip Arthroplasty by Means of Computed Tomography 3D Models and Fracture Risk Evaluation. Artif Organs 2013; 37:567-573. DOI: 10.1111/aor.12033.

[53] Kalender WA, Hebel R, Ebersberger J. Reduction of CT artifacts caused by metallic implants. Radiology. 1987; 164:576-7.

[54] Andersson KM, Nowik P, Persliden J, Thunberg P, Norrman E. Metal artefact reduction in CT imaging of hip prostheses-an evaluation of commercial techniques provided by four vendors. Br J Radiol. 2015; 88:20140473. DOI: 10.1259/bjr.20140473

[55] Boas FE, Fleischmann D. Evaluation of two iterative techniques for reducing metal artefacts in computed tomography. Radiology. 2011; 259(3): 894-902. DOI: 10.1148/radiol.11101782

[56] 3D Slicer, available: http://www.slicer.org, accessed: 2018 May15.
[57] Rahunathan S, Stredney D, Schmalbrock P, Clymer BD. Image Registration Using Rigid Registration and Maximization of Mutual Information. The 13th Annual Medicine Meets Virtual Reality Conference. 2005 January 26–29; Long Beach, CA.
[58] Engh CA, McGovern TF, Bobyn JD, Harris WH. A quantitive evaluation of periprosthetic bone remodeling after cementless total hip arthroplasty. J Bone Joint Surg Am. 1992; 74:1009-20.
[59] Ang KC, Das De S, Goh JC, Low SL, Bose K. Periprosthetic bone remodeling after cementless total hip replacement: a prospective comparison of two different implant designs. J Bone Joint Surg Br. 1997; 89:675-9.
[60] McCarthy CK, Steinberg GG, Agren M. Quantifying bone loss from the proximal femur after total hip arthroplasty. J Bone Joint Surg Br. 1991; 73:774-8.
[61] Karachalios T, Tsatsaronis C, Efraimis G, Papadelis P, Lyritis G, Diakoumopoulos G. The long-term clinical relevance of calcar atrophy caused by stress shielding in total hip arthroplasty: a 10-year, prospective, randomized study. J Arthroplasty. 2004;19(4):469-75. DOI: 10.1016/j.arth.2003.12.081